

Even more definitive evidence regarding the preferred conformation of bidentate chelates derived from **2** was obtained for the case of  $\text{MgBr}_2$  as Lewis acid; a discrete bidentate chelate with very narrow  $^1\text{H}$  NMR lines was observed at 0 °C. Irradiation of the methyl group collapsed the six-line multiplet for the  $\text{C}_3$  methine to a triplet with  $J = 5$  Hz. These results require that the  $\text{C}_3$  C–H bond essentially bisects the H–C–H angle at C-2, i.e., that the methyl group at  $\text{C}_3$  occupies an axial (or pseudoaxial) orientation in the complexes formed from **2** and  $\text{TiCl}_4$  or  $\text{MgBr}_2$ .<sup>10</sup>

It is now clear why “chelation-controlled” additions to **2** are characterized by high levels of diastereofacial selectivity. Apparently, relief of  $\text{A}^{1,3}$ -like interactions between the  $\text{C}_3$  methyl group and the benzyl group on oxygen is responsible for the conformation of chelates derived from **2** in solution; no significant 1,3-diaxial interactions are present to disfavor this conformation. For the first time, the stereochemistry of Lewis acid mediated additions to materials such as **1** and **2** can be interpreted on a rational basis—one based upon experiment rather than hypothesis.

**Acknowledgment.** This research was supported by the National Institutes of Health (through Grant GM-28961), to whom we are most grateful. We also thank the National Institutes of Health, the National Science Foundation, and the University of Utah Institutional Funds Committee for funding for the purchase of the spectrometer used in this work.

(10)  $^1\text{H}$  NMR chemical shifts for the complexes formed from **2** with  $\text{MgBr}_2\text{-OEt}_2$  and  $\text{TiCl}_4$  are summarized here, as are chemical shift differences relative to **2** at the same temperature (12.3 and –93 °C, respectively):  $\text{MgBr}_2\text{-C}_1$  9.85 (–0.13),  $\text{C}_2$ ,  $\text{C}_2$  2.91 (–0.30, –0.44),  $\text{C}_3$  4.11 (–0.08),  $\text{C}_4$  4.65 (–0.24),  $\text{C}_4$  4.79 (–0.24),  $\text{CH}_3$  1.23 (0.01);  $\text{TiCl}_4\text{-C}_1$  10.10 (–0.39),  $\text{C}_2$ ,  $\text{C}_2$  3.41 (–0.91),  $\text{C}_3$  4.73 (–0.70),  $\text{C}_4$  5.28 (–0.73),  $\text{C}_4$  5.46 (–0.91),  $\text{CH}_3$  1.21 (0.03).

(11) (a) The aldehydic proton is omitted for clarity. (b) Only the indicated relationships at  $\text{C}_2$  and  $\text{C}_3$  are stereochemically significant.

### Neutron Diffraction Evidence for Unusual Cohesive H-Bonding Interactions in $\beta$ -(BEDT-TTF) $_2\text{X}$ Organic Superconductors

T. J. Emge, H. H. Wang, U. Geiser, M. A. Beno, K. S. Webb, and Jack M. Williams\*

Chemistry and Materials Science and Technology Divisions  
Argonne National Laboratory, Argonne, Illinois 60439

Received March 11, 1986

In order to determine the nature and exact geometries of the interionic interactions that are responsible for crystal cohesion between the sheetlike networks of radical cation molecules and the halide-containing anions in the layered organic conductors of the type  $\beta$ -(ET) $_2\text{X}$ ,<sup>1</sup> we have undertaken low-temperature (20 K) neutron diffraction studies of the  $\text{X}^- = \text{AuI}_2^-$  and  $\text{I}_3^-$  salts. For these synthetic organic superconductors,  $\beta$ -(ET) $_2\text{AuI}_2$  has the highest  $T_c$  (~5 K) at ambient pressure,<sup>2,3</sup> and  $\beta$ -(ET) $_2\text{I}_3$  has the highest  $T_c$  (~8 K) under a nonhydrostatic pressure of 1.3 kbar.<sup>4-6</sup>

\* Author to whom correspondence should be addressed.

(1) The abbreviations “ET” and “BEDT-TTF” refer to the organic donor molecule bis(ethylenedithio)tetrathiafulvalene ( $\text{C}_{10}\text{H}_8\text{S}_8$ ) as in: Mizuno, M.; Garito, A. F.; Cava, M. P. *J. Chem. Soc., Chem. Commun.* **1978**, 18.

(2) Wang, H. H.; Beno, M. A.; Geiser, U.; Firestone, M. A.; Webb, K. S.; Nuñez, L.; Crabtree, G. W.; Carlson, K. D.; Williams, J. M.; Azevedo, L. J.; Kwak, J. F.; Schirber, J. E. *Inorg. Chem.* **1985**, *24*, 2465.

(3) Carlson, K. D.; Crabtree, G. W.; Nuñez, L.; Wang, H. H.; Beno, M. A.; Geiser, U.; Firestone, M. A.; Webb, K. S.; Williams, J. M. *Solid State Commun.* **1986**, *57*, 89.

(4) Murata, K.; Tokumoto, M.; Anzai, H.; Bando, H.; Saito, G.; Kajimura, K.; Ishiguro, T. *J. Phys. Soc. Jpn.* **1985**, *54*, 1236.

(5) Laukhin, V. N.; Kostyuchenko, E. E.; Sushko, Yu. B.; Shchegolev, I. F.; Yagubski, E. B. *JETP Lett. (Engl. Transl.)* **1985**, *41*, 81.

**Table I.** H-Bonding Interaction Geometries for Several  $\beta$ -(ET) $_2\text{X}$  Salts Derived from 20 K Neutron Data and Low-Temperature X-ray Data<sup>a</sup>

$\text{X}^- = \text{AuI}_2^-$ , 20 K neutrons			$\text{X}^- = \text{AuI}_2^-$ , 120 K X-rays		
contact	dist/Å	angle/deg	dist/Å	angle/deg	
H102...I	2.966 (4)	147.8 (3)	3.03	141.8	
H81...I	3.132 (4)	148.3 (3)	3.13	153.9	
H71...I	3.146 (4)	122.6 (3)	3.20	120.0	
H92...I	3.154 (4)	136.6 (3)	3.27	129.6	
H102...I	3.222 (4)	123.3 (3)	3.24	127.2	
$\text{X}^- = \text{I}_3^-$ , 20 K neutrons <sup>15</sup>			$\text{X}^- = \text{I}_3^-$ , 9 K X-rays		
contact	dist/Å	angle/deg	dist/Å	angle/deg	
H81...I	3.082 (7)	140.9 (6)	3.03	147.3	
H82...I	3.179 (7)	131.1 (6)	3.17	131.6	
$\text{X}^- = \text{IBr}_2^-$ , 9 K X-rays			$\text{X}^- = \text{ICl}_2^-$ , 120 K X-rays		
contact	dist/Å	angle/deg	contact	dist/Å	angle/deg
H102...Br	2.89	132.7	H71...Cl	2.59	168.2
H81...Br	2.90	154.4	H102...Cl	2.63	167.2
H102...Br	2.94	136.3	H91...Cl	2.77	129.9
H82...Br	3.14	126.8	H81...Cl	2.88	117.1
H92...Br	3.18	128.2	H92...Cl	2.91	140.5

<sup>a</sup>The observed C–H bond distances derived from our neutron diffraction data average 1.09 (1) Å. For the X-ray results, the H atom coordinates were calculated by using C–H bond distances of 1.09 Å and  $\text{sp}^3$  geometries.

It has been shown that a direct relationship exists between the two-dimensional (2D) electrical behavior and the crystal structures of the  $\beta$ -(ET) $_2\text{X}$  salts, because of their sheetlike networks of strongly interacting ET molecules.<sup>7-9</sup> However, the crystal packing interactions between the 2D ET molecule networks and the adjacent, parallel layers of  $\text{X}^-$  anions are not well understood. The donor–anion interactions may be bonding (i.e., attractive), as expected for Coulombic interactions between counterions, or nonbonding (i.e., repulsive), as previously found for donor–donor interactions in  $\beta$ -(ET) $_2\text{X}$  salts based upon theoretical calculations.<sup>9</sup> Also, the donor–anion interactions in the modulated phase<sup>15</sup> of  $\beta$ -(ET) $_2\text{I}_3$  ( $T < 200$  K) appear to be correlated to the modulation, which is unique in that  $\beta$ -(ET) $_2\text{I}_3$  contains the largest triatomic anion,  $\text{I}_3^-$ , in this series of materials. Of particular importance to the investigation of donor–anion interactions in these salts is the precise description of significant intermolecular contacts. The relationship between electrical properties and anion size for the  $\beta$ -(ET) $_2\text{X}$  conductors, where  $\text{X}^-$  is a linear triatomic anion, is examined here in terms of the donor–anion interactions.

Because of the molecular environment at the interface between the ET molecule network and the anion layer in  $\beta$ -(ET) $_2\text{X}$  salts, the only short intermolecular contacts between ET donors and  $\text{X}^-$  anions (i.e., interatomic distances less than the sum of the van der Waals radii<sup>10</sup>) are of the H...X type. Thus, it is imperative to obtain precise H atom positions, which can be derived only from neutron diffraction data, to accurately compare the donor–anion interactions for the various  $\beta$ -(ET) $_2\text{X}$  superconductors. The approximate coordination of five nearby H atoms to each terminal halide atom of the  $\text{X}^-$  anion is observed by use of neutron or X-ray data for all of the superconducting  $\beta$ -(ET) $_2\text{X}$  salts.<sup>11,12</sup> In these

(6) Schirber, J. E.; Azevedo, L. J.; Kwak, J. F.; Venturini, E. L.; Leung, P. C. W.; Beno, M. A.; Wang, H. H.; Williams, J. M. *Phys. Rev. B* **1987**, *33*, (7) Mori, T.; Kobayashi, A.; Sasaki, Y.; Kobayashi, H.; Saito, G.; Inokuchi, H. *Chem. Lett.* **1984**, 957.

(8) Whangbo, M.-H.; Williams, J. M.; Leung, P. C. W.; Beno, M. A.; Emge, T. J.; Wang, H. H.; Carlson, K. D.; Crabtree, G. W. *J. Am. Chem. Soc.* **1985**, *107*, 5815.

(9) Whangbo, M.-H.; Williams, J. M.; Leung, P. C. W.; Beno, M. A.; Emge, T. J.; Wang, H. H. *Inorg. Chem.* **1985**, *24*, 3500.

(10) For the van der Waals radii used here (2.15 Å for I, 1.95 Å for Br, 1.80 Å for Cl, and 1.20 Å for H), see: Pauling, L. *The Nature of the Chemical Bond*, 3rd ed.; Cornell University Press: Ithaca, New York, 1960; p 260.

(11) Emge, T. J.; Leung, P. C. W.; Beno, M. A.; Wang, H. H.; Firestone, M. A.; Webb, K. S.; Carlson, K. D.; Williams, J. M.; Venturini, E. L.; Azevedo, L. J.; Schirber, J. E. *Mol. Cryst. Liq. Cryst.* **1986**, *132*, 363.

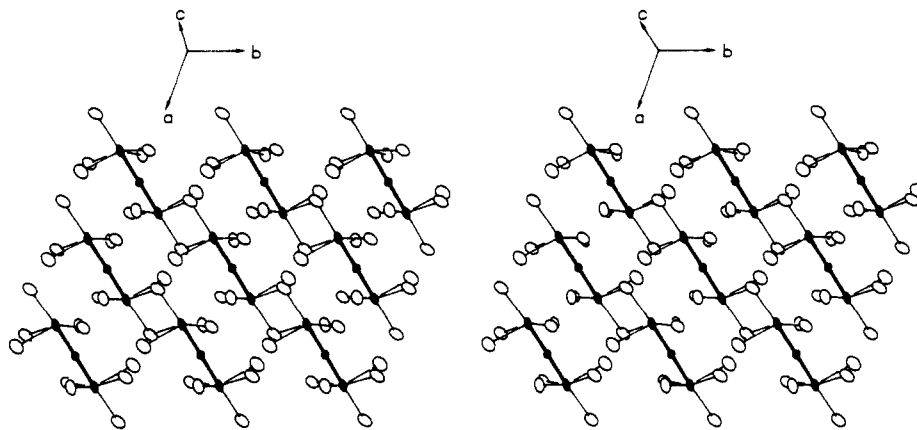


**Figure 1.** A stereoview of the  $ab$  plane of  $\beta$ -(ET) $_2$ AuI $_2$  at 20 K shows the AuI $_2^-$  anions and the numerous short H $\cdots$ I contacts (thin lines) with distances less than the van der Waals radii sum of 3.3 Å. The environment about each terminal I atom of the anions is nearly an octahedron of atoms. Thermal ellipsoids are known very precisely and are drawn at the 99% probability level.<sup>16</sup>

materials, there is a nearly octahedral environment of atoms about the terminal halogen atoms of the anion (see Figure 1). The shortest H $\cdots$ X distances and their corresponding C-H $\cdots$ X angles for several  $\beta$ -(ET) $_2$ X salts with X $^-$  = linear anion are given in Table I. Although the most precise geometries in Table I are those obtained from neutron diffraction data, the low-temperature X-ray results agree surprisingly well, by comparison. Thus, the neutron diffraction experiments *verify* previous assumptions concerning the H $\cdots$ X geometries based upon low-temperature X-ray diffraction data. The H atom geometries that were calculated for the completely ordered structures of  $\beta$ -(ET) $_2$ IBr $_2$ <sup>11</sup> and  $\beta$ -(ET) $_2$ ICl $_2$ <sup>12</sup> from low-temperature X-ray data are also expected to be accurate (by comparison) and these parameters are included in Table I. The differences in the H $\cdots$ X interactions of the  $\beta$ -(ET) $_2$ X salts with X $^-$  = AuI $_2^-$ , IBr $_2^-$ , and ICl $_2^-$  are summarized as follows: (i) for the shortest H $\cdots$ X contacts in the above three salts, the angles about the H atoms, namely C-H $\cdots$ I, C-H $\cdots$ Br, and C-H $\cdots$ Cl, are largest for  $\beta$ -(ET) $_2$ ICl $_2$  (approaching 180°) and are smallest for  $\beta$ -(ET) $_2$ AuI $_2$ ; (ii) for longer contact distances in each of the above salts, the corresponding C-H $\cdots$ X angles are much smaller (i.e., approaching 120°); (iii) the H $\cdots$ Br, and H $\cdots$ Cl contact distances are as much as 0.38, 0.26, and 0.41 Å *shorter* than their respective van der Waals radii sums,<sup>10</sup> which is significant in comparison to the estimated errors for the values of the H $\cdots$ X distances derived from X-ray data ( $\pm 0.1$  Å or less). The above structural results confirm that the closest H $\cdots$ X contacts in the  $\beta$ -(ET) $_2$ X salts are the main contributors to the cohesive forces between the 2D ET molecule networks and the anions in these crystals and that these H $\cdots$ X interactions are similar to H-bonding interactions in other organic compounds.<sup>13,14</sup> The discovery of the very short H $\cdots$ I contacts in  $\beta$ -(ET) $_2$ AuI $_2$  is surprising because such interactions are generally assumed to be weak.<sup>13,14</sup> In summary, there are important implications for the design and synthesis of new  $\beta$ -(ET) $_2$ X systems where the X $_n^-$  anions contain halide (I, Br, Cl, F) atoms, namely, that H-bonding interactions of the type H $\cdots$ X play a major role in determining the

crystal cohesive forces between donors and anions thereby controlling compound formation.

**Acknowledgment.** Work was carried out at Argonne National Laboratory under Contract W-31-109-ENG-38 and at the High Flux Beam Reactor (HFBR), Brookhaven National Laboratory, under Contract DE-AC02-76CH00016 and is supported by the U.S. Department of Energy. T.J.E. is a research collaborator with the Chemistry Department, Brookhaven National Laboratory. K.S.W. is an undergraduate research participant sponsored by the Argonne Division of Educational Programs from St. Michael's College, Winooski, VT. We thank J. Henriques for his expert technical assistance and T. F. Koetzle and R. K. McMullan for their assistance and helpful discussions.

**Supplementary Material Available:** Table S1, neutron data collection and refinement parameters; Table S2, atomic positional and thermal parameters for  $\beta$ -(ET) $_2$ AuI $_2$  at 20 (neutron data) and 120 K (X-ray data); Table S3, atomic positional and thermal parameters for  $\beta$ -(ET) $_2$ I $_2$  at 20 (neutron data) and 9 K (X-ray data); Table S4, atomic positional and thermal parameters for  $\beta$ -(ET) $_2$ IBr $_2$  at 9 K (X-ray data) (6 pages). Ordering information is given on any current masthead page.

### Polyhedral Oligometallasilsesquioxanes (POMSS) as Models for Silica-Supported Transition-Metal Catalysts: Synthesis and Characterization of (C $_5$ Me $_5$ )Zr[(Si $_7$ O $_12$ )(c-C $_6$ H $_{11}$ ) $_7$ ]

Frank J. Feher

Department of Chemistry, University of California  
Irvine, California 92717

Received March 12, 1986

Heterogeneous silica-supported transition-metal compounds play an increasingly important role as catalysts in the petrochemical industry.<sup>1</sup> The commercial importance of such catalysts has stimulated an intense interest in the chemical processes which occur on the surface of heterogeneous catalysts. Although recent

(12) Emge, T. J.; Wang, H. H.; Leung, P. C. W.; Rust, P. R.; Cook, J. D.; Jackson, P. L.; Carlson, K. D.; Williams, J. M.; Whangbo, M.-H.; Venturini, E. L.; Schirber, J. E.; Azevedo, L. J.; Ferraro, J. R. *J. Am. Chem. Soc.* **1986**, *108*, 695.

(13) Hamilton, W. C.; Ibers, J. A. *Hydrogen Bonding in Solids*; W. A. Benjamin: New York, 1968; pp 14-21.

(14) Taylor, R.; Kennard, O. *Acc. Chem. Res.* **1984**, *17*, 320.

(15) The structure of  $\beta$ -(ET) $_2$ I $_2$  becomes modulated below  $\sim 200$  K at ambient pressure, and the average (i.e., sublattice) structure is used here. Also, the distances to the C(9)-C(10) ethylene group of the ET molecule in  $\beta$ -(ET) $_2$ I $_2$  have two entries in Table I, since this group is disordered. For the modulated structure of  $\beta$ -(ET) $_2$ I $_2$ , see: (a) Leung, P. C. W.; Emge, T. J.; Beno, M. A.; Wang, H. H.; Williams, J. M.; Petricek, V.; Coppens, P. *J. Am. Chem. Soc.* **1985**, *107*, 6184. (b) Leung, P. C. W.; Emge, T. J.; Beno, M. A.; Wang, H. H.; Williams, J. M.; Petricek, V.; Coppens, P. *J. Am. Chem. Soc.* **1984**, *106*, 7644.

(16) Johnson, C. K. ORTEP 1965, Report ORNL-3794, Oak Ridge National Laboratory, Oak Ridge, TN.

(1) (a) Yermakov, Y. I.; Kuznetsov, B. N.; Zakharov, V. A. *Catalysis by Supported Complexes*; Elsevier: New York, 1981. (b) Seiyama, T.; Tanabe, K., Eds. *New Horizons in Catalysis*; Elsevier: New York, 1980. (c) Thomas, C. *Catalytic Processes and Proven Catalysts*; Academic Press: New York, 1970. (d) Pearce, R.; Patterson, W. R. *Catalysis and Chemical Processes*; Blackie and Son: Glasgow, 1981. (e) Golodets, G. I. *Heterogeneous Catalytic Reactions Involving Molecular Oxygen*; Elsevier: New York, 1983.